IEEE/CSC & ESAS EUROPEAN SUPERCONDUCTIVITY NEWS FORUM (ESNF), No. 10, October 2009.
Published in *AIP Conference Proceedings* **1219**, pp. 239-246 (2010)

BENDING EFFECTS ON CRITICAL CURRENTS OF Nb_3Sn SUPERCONDUCTING WIRES

M. Takayasu[1], L. Chiesa[2], J. H. Schultz[1], and J. V. Minervini[1]

[1]Massachusetts Institute of Technology
Cambridge, MA, 02139, USA

[2]Tufts University
Medford, MA, 02155, USA

ABSTRACT

Bending effects on Nb_3Sn wires have been investigated to understand the critical current degradation of large Nb_3Sn superconducting cables. An integrated model taking into accounts the neutral axis shift, the current transfer length, the mechanical filament breakage and the uniaxial strain release due to applying bending has been developed. Five different Nb_3Sn wires, developed by the ITER parties, were tested. The experimental data are presented and analyzed with a newly developed integrated model. The current transfer effect shows to be an important factor.

KEYWORDS: Bending strain, neutral axis shift, current transfer, filament breakage, Nb_3Sn superconductor.

INTRODUCTION

The effects of bending on the critical current behavior of superconduting strands are investigated. Bending phenomena of Nb_3Sn wires were experimentally characterized using a previously reported variable pure-bending strand test device [1]. The critical currents were measured over a wide range of bending, up to the nominal bending strain of 0.8% at the outer strand surface. Irreversible degradation of the critical currents due to bending was also evaluated. Five Nb_3Sn wires, developed by the ITER parties, were tested. The experimental data were evaluated with a newly developed integrated model using the existing uniaxial strain data of the wires. The model takes into account four different effects: the neutral axis shift, the current transfer length, the mechanical filament breakage and the uniaxial strain release due to applied bending.

MODEL ANALYSIS

Critical Current Formula

To analyze the critical current of the bending effects, the scaling formula recommended recently by Bottura [2] was used. The critical current density is given:

$$J_c = \frac{C}{B} s(e)(1-t^{1.52})(1-t^2)b^p(1-b)^q \quad (1)$$

where $s(\varepsilon) = 1 + \left[C_{a1}\left(\sqrt{\varepsilon_{sh}^2 + \varepsilon_{0a}^2} - \sqrt{(\varepsilon - \varepsilon_{sh})^2 + \varepsilon_{0a}^2}\right) - C_{a2}\varepsilon \right] \Big/ (1 - C_{a1}\varepsilon_{0a})$, $\varepsilon_{sh} = C_{a2}\varepsilon_{0,a} \Big/ \sqrt{C_{a1}^2 - C_{a2}^2}$, $b = B \big/ B_{C2}^*(T, \varepsilon)$, $b_0 = B \big/ B_{C2}^*(0, \varepsilon)$, $t = T \big/ T_C^*(0, \varepsilon)$, $T_C^*(B, \varepsilon) = T_{C0\max}^* [s(\varepsilon)]^{\frac{1}{3}} (1 - b_0)^{\frac{1}{1.52}}$, $B_{C2}^*(T, \varepsilon) = B_{C20\max}^* s(\varepsilon)(1 - t^{1.52})$, C = The scaling constant, $B_{C20\max}^*$ = The upper critical field at zero temperature and strain, $T_{C0\max}^*$ = The critical temperature at zero field and strain, p = The low field exponent of the pinning force ($p < 1$, $p \approx 0.5$), q = The high field exponent of the pinning force ($q \approx 2$), C_{a1}=The strain fitting constant, C_{a2}=The strain fitting constant, ε_{0a} = The residual strain component, $\varepsilon_{\max}$ = The tensile strain at which the maximum critical properties are reached.

Conventional Model of Bending Effects on Strand Critical Current

The critical current of a multi-filamentary twisted superconducting strand under bending strains has been formulated by Ekin [3], and his concept has been adopted for various works [4]-[7]. Ekin considered critical current transfer between filaments due to axial strains under bending in a twisted strand. Two extreme cases have been considered; long twist pitch (low inter-filament resistivity), and short twist pitch (high inter-filament resistivity). We will call the former case "Perfect Current Transfer," and the latter "No Current Transfer."

Perfect current transfer: If currents can transfer between filaments without electric loss (zero transverse resistance), the critical current of a multifilamentary strand can be obtained from the total current of one cross-section of a strand [3] and is given by

$$I_c = 2\int_{-R_{nc}}^{R_{nc}} j_c(\varepsilon_y)\sqrt{R_{nc}^2 - y^2}\, dy \quad (2)$$

here, R_{nc}=The non-copper area radius, $\varepsilon_y = \varepsilon_0 + \varepsilon_{by}$, ε_0 = The precompressive strain, $\varepsilon_{by} = y/R_b$.

No current transfer: If the transverse resistance between filaments is high enough and no current can transfer between filaments, the critical current of each filament can be limited by the worst point in one twist pitch with regard to bending strain distributions. Therefore the current of a strand is given by [3]

$$I_c = 2\pi\int_0^{R_{nc}} j_c(\varepsilon_y) y\, dy \quad (3)$$

here, $\varepsilon_y = \varepsilon_0 + \varepsilon_{by}$, $\varepsilon_{by} = -y/R_b$ for $j_c(\varepsilon_0 - y/R_b) < j_c(\varepsilon_y + y/R_b)$, or $\varepsilon_{by} = +y/R_b$ for $j_c(\varepsilon_0 - y/R_b) > j_c(\varepsilon_y + y/R_b)$. Note that the worst point of the critical current does not occur always at the compression side. At a large bending rate the tension side may happen to create larger degradation of the critical current than the compression side since the critical current decreases at the tension side more sharply than at the compression side. To account for this effect we introduce an minimum function operator to express a minimum value of $j_c(\varepsilon)$ in the range of strains between $-\varepsilon_{by}$ and $+\varepsilon_{by}$, and we rewrite equation (3) as:

$$I_c = 2\pi\int_0^{R_{nc}} \left\{ \min\left| j_c(\varepsilon_y) \right|_{\varepsilon_y = \varepsilon_0 - \varepsilon_{by}}^{\varepsilon_y = \varepsilon_0 + \varepsilon_{by}} \right\} y\, dy \quad (4)$$

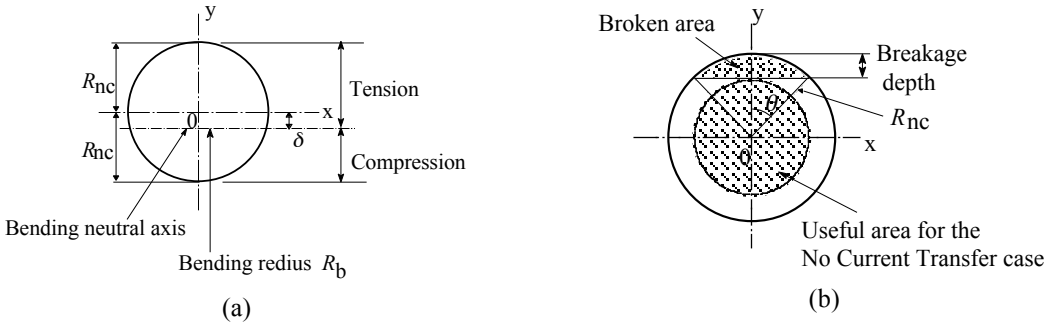

FIGURE 1. Cross-section of non-copper showing the neutral axis shift of δ (left), and schematic of non-copper area having broken filament area (right).

Integrated Model

In general the experimental results of the critical currents under a wide range of bending strains have been known to fit neither the Perfect Current Transfer model nor the No Current Transfer model. Our experimental results show only a good fit to the Perfect Current Transfer model at small bending rates, and then sharply drop off toward the prediction line of No Current Transfer model with increasing bending. We have investigated four effects due to mechanical bending, that is, the neutral-axis shift [3], [8], [9], the current transfer length, the filament breakage [10], and the uniaxial strain releasing [8], [11]. FIGURE 1 shows the strand cross-section views to illustrate the neutral-axis shift model (left) and the filament breakage model (right).

Neutral-Axis Shift Effect: A shift of the neutral-axis due to yielding of the strand matrix under bending has been pointed out by Ekin [3]. When the neutral-axis shifts toward the compressive side by δ as shown in FIGURE 1 left. The bending strain ε_{by} is given by

$$\varepsilon_{by} = (y+\delta)/(R_b-\delta) \tag{5}$$

The peak bending strains of the filament on the tension and compression sides are written as $\varepsilon_{bp}^{+} = (R_{nc}+\delta)/(R_b-\delta)$ and $\varepsilon_{bp}^{-} = -(R_{nc}-\delta)/(R_b-\delta)$, respectively.

The critical current for Perfect Current Transfer and No Current Transfer can be obtained using equation (5) by equations (2) and (4), respectively. All integrations were carried out by the Gaussian integration method of order 40 using Microsoft Excel®.

FIGURE 2 shows the calculated neutral-axis shift effects on the critical current for the Perfect Current Transfer and No Current Transfer cases, respectively. In the Perfect Current Transfer case the critical current shows a maximum peak at certain conditions since the tension area increases. This was observed for the Furukawa wire (FIGURE 9).

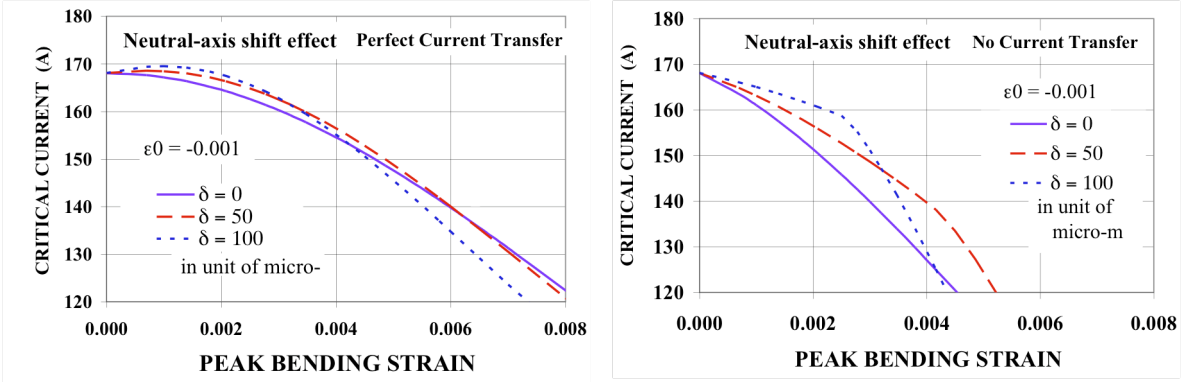

FIGURE 2. Calculated critical currents of neutral-axis shift effect for Perfect Current Transfer (left), and calculated critical currents of neutral-axis shift effect for No Current Transfer (right).

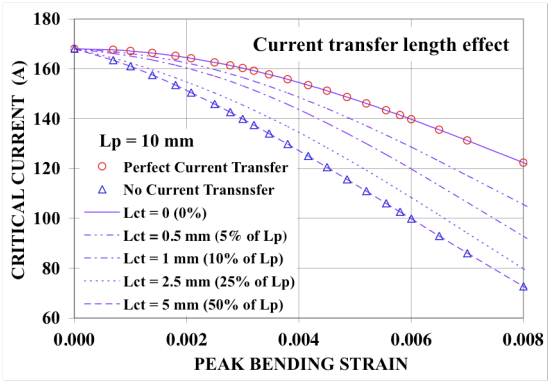

FIGURE. 3 Calculated critical currents of current transfer effect with various current transfer length.

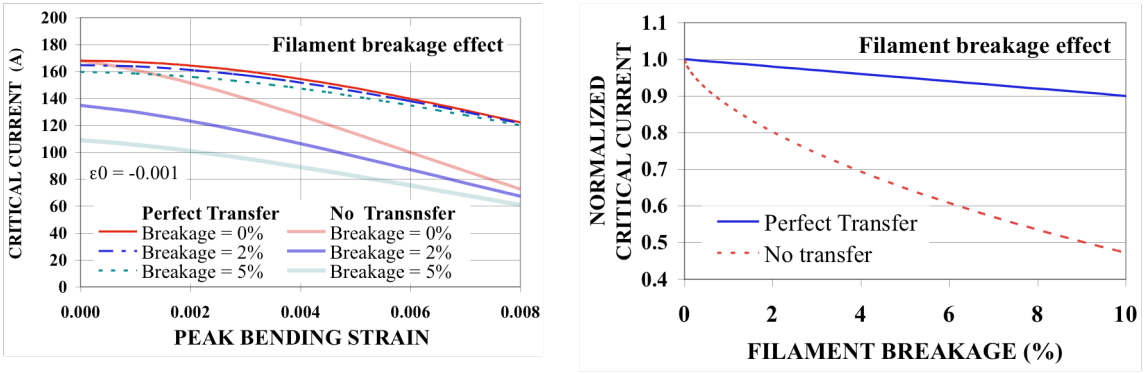

FIGURE 4 Calculated critical currents of the filament breakage effect of Perfect Current Transfer (dotted lines) and No Current Transfer (bold lines) cases for the breakage fractions of 0%, 2% and 5% (left). Critical current degradations due to the breakage at zero bending for Perfect Current Transfer and No Current Transfer (right).

Current Transfer Length Effect: The current transfer length affects the total critical currents with regard to the twist pitch length L_p. The current transfer length L_{ct} has been given as a function of the transverse resistance of matrix material between filaments and the n-value of the resistive transition of the superconductor by [6], [12], [13],

$$L_{ct} \approx d\sqrt{\frac{0.106}{n}\frac{\rho_m}{\rho^*}} \tag{6}$$

here, n = The empirical power factor ($\rho = kJ^n$) representing the resistive transition in the superconductor, ρ_m = The transverse resistance of the matrix between filaments, ρ^* = The superconductor resistivity criterion of the critical current, d = The conductor diameter[12]. Sometimes the strand diameter has been used for d [6], however the diameter d is a measure with regard to the current transfer spacing between filaments, therefore d could be much smaller than the strand diameter. Regardless of the accuracy of the current transfer length itself, the relative ratio of the current transfer length to the twist pitch (L_{ct} / L_p) is an important factor for characterizing the current transfer effects on the critical current.

To take into account the current transfer effect, the critical current of a filament at a given point z along a filament is assumed to be dominated by the minimum critical-current value between z - L_{ct}/2 and z + L_{ct}/2. Now the critical current can be given using the minimum function operator defined for equation (4) as in cylindrical coordinates,

$$I_c = 2\int_0^{R_{nc}} \int_{-\frac{\pi}{2}}^{\frac{\pi}{2}} \left\{ \min\left| j_c(\varepsilon_{r\phi}) \right|_{\phi=\varphi-\varphi_{ct}}^{\phi=\varphi+\varphi_{ct}} \right\} r\, d\varphi\, dr \tag{7}$$

where, $\varepsilon_{r\phi} = \varepsilon_0 + \varepsilon_{br\phi}$, $\varepsilon_{br\phi} = r\sin\phi/R_b$, $\varphi_{ct} = 2\pi L_{ct}\sin\theta/L_p$, and $\theta = \tan^{-1}\left(L_p/2\pi R_{nc}\right)$, L_{ct} =The minimum current transfer length, and L_p =The twist pitch length of strand.

FIGURE 3 shows the calculated critical currents with various current transfer lengths L_{ct} of 0.5 mm, 1 mm, 2.5 mm and 5 mm for a strand with the twist pitch L_p = 10 mm. These L_{ct} values correspond to 0, 5%, 10%, 25% and 50% of the twist pitch length. The curves of L_{ct} = 0 and L_{ct} = 0.5 L_p agree with the results of Perfect Current transfer (open circle) and No Current transfer (open triangle), respectively.

Filament Breakage Effect: Filament breakages in the tension side due to bending have been found [10]. Such filament breakage is probably the dominant cause of the irreversible permanent degradation. If the filament breakage occurs near the surface of the tension side as shown in FIGURE 1 right, the critical currents can be obtained with integration over the unbroken area for the Perfect Current Transfer case. However in the case of No Current Transfer the effective superconducting filaments are only in the center circular section which does not overlap the broken area, since the strand is twisted (FIGURE 1 right).

FIGURE 4 right shows the calculated critical currents of the filament breakage for the Perfect Current Transfer (dotted lines) and No Current Transfer (bold lines) cases with the breakage area fractions of 0%, 2% and 5%. In the case of Perfect Current Transfer, critical current degradations are the same rates as that of the breakages. On the other hand the degradations of the No Current Transfer case are significant, for example about 35% for the 5% breakage even at zero bending (FIGURE 4 left).

Uniaxial Strain Releasing Effect: Uniaxial thermally induced precompressive strain during cooldown after reaction of a Nb_3Sn wire could be released by mechanical bending cycles [11]. The result is that the strain $|\varepsilon_{max}|$ becomes smaller and the critical current increases. The increase of the critical current at zero bending after bending cycles could be driven only by this strain releasing effect. In the present experiments this effect seemed to be very small, but to happen for some wires.

EXPERIMENTAL

The bending tests were carried out using our variable bending test device developed and described earlier. The device can apply a large range of bending, in liquid helium, to a strand sample of about 100 mm length, up to 0.8% of the nominal bending strain at the surface of a wire of 0.8 mm diameter. Details of the device have been described in [1].

We tested five different Nb_3Sn wires which were developed by the ITER parties. Three were internal-tin wires of recently developed ITER TF US Oxford and Luvata wires, and EU EM-LMI wire. Two of them were bronze wires of EU European Advanced Superconductors (EAS) and Japanese Furukawa designs, developed during the ITER Engineering Design Activity of the 1990's. Test wire characteristics and their heat-treatment schedules are seen as well as details of experimental results in [14]. The bending tests were performed at 12 T or 15 T in liquid helium using the 20 T, 195 mm Bitter magnet at NHMFL, Florida State University. The test results are shown in the following section.

DISCUSSION

To use the scaling law of equation (1) for analyses of the experimental results, parameters required for the equation were selected on the bases of various published work [5], [15]-[17]. Few parameters for the wires presented in this work were not available so they were adjusted by our measured critical current results of magnetic field dependences. The parameters used for the tested wires are summarized in Table 1. The parameters of p

and q were p=0.5 and q=2. The parameters might not be accurate. However the results of the model analyses are not strongly affected by modest changes of the parameters.

Table 1 Scaling parameters in equation 1 used for tested wires.

Strand	Oxford	Luvata	EAS	EM-LMI	Furukawa
B^*_{c20max} (T)	32.5	32.5	35.75	28.7	32.5
T^*_{c0max} (K)	17.8	17.0	16.52	16.89	16.5
C (AT)	18500	17000	14150	12750	11500
ε_{0a}	0.00344	0.0034	0.0025	0.0019	0.0020
ε_{max}	0.0005	0.0011	0.0024	0.0011	0.0023
C_{a1}	53.3	60.0	71.39	45.16	44.35
C_{a2}	8.55	20.0	28.28	8.45	12.25

The critical current behavior of each tested wire for bending strains was unique as shown below. The critical current trends with the bending strains were analyzed by selecting the best fitting parameters of the four effects using a curve fitting method.

Curve fitting results for the Oxford sample are shown in FIGURE 5a. Experimental results are shown with solid circles as a function of the peak bending strain of the filament which is the maximum bending at the outer most filaments. The measured data lie between curves obtained from the Perfect Current Transfer model (upper line line) and the No Current Transfer model (lower thin line). The bold line was obtained by taking account of the four effects; the neutral axis shift, the current transfer length, the filament breakage and the uniaxial strain releasing, in order to fit the experimental data. Each parameter of the four effects used for the fittings are shown as a function of the bending strain in FIGURE 5a. Three dotted lines in FIGURE 5 show calculated recovery curves of the critical currents after the peak bendings of 0.42%, 0.49% and 0.56%, respectively. The recovered critical currents at zero bending agree well with the experimental results. The Oxford wire sample showed significant irreversible permanent degradation, which could be explained with 2% filament breakage at 0.56% of the peak bending strain.

FIGURE 5b shows the curve fitting results of a Luvata wire sample. The sharp decrease of the critical current above 0.45% bendings was reflected by the sharp increase of the current transfer length. Permanent degradation of the Luvata sample was negligible, implying an absence of filament breakage. FIGURE 5c shows the curve fitting results of an EU EAS wire sample. The EAS wire sample showed very small bending effects. The critical current increases slightly with increasing bending strains. This probably is the result of neutral axis shifts. FIGURE 5d shows the curve fitting results of an EU EM-LMI wire sample. The internal tin EM-LMI sample showed bending effects as large as other internal tin wires of Oxford and Luvata wires. Permanent degradation of this wire was small, similar to the Luvata wire. FIGURE 5e shows the curve fitting results of a Furukawa wire sample. The 1% increase of the critical current for the Furukawa wire sample at 0.3% peak bending can be simulated by assuming a 70 μm shift of the neutral axis. Three dotted lines show recovery curves of the critical currents after the given bendings of 0.37%, 0.44% and 0.50%. The maximum of the critical currents at about 0.3% peak bending and also the recovered critical currents at zero bending agree well with the experimental results.

Each of the four effects; the neutral axis shift, the current transfer length, the breakage and the thermally induced strain release had very unique contribution to the critical currents respectively, so that the four fitting parameters of them were relatively easily determined. However, the resulted parameters for the five samples might not be definitive determinations. The calculated neutral axis shifts for all of the samples were quite large. Further investigations of the mechanical dynamics of the superconducting matrixes during bending are recommended. The recovery behavior of the critical currents after applying bending is very useful to understanding the effects of bending on the critical currents.

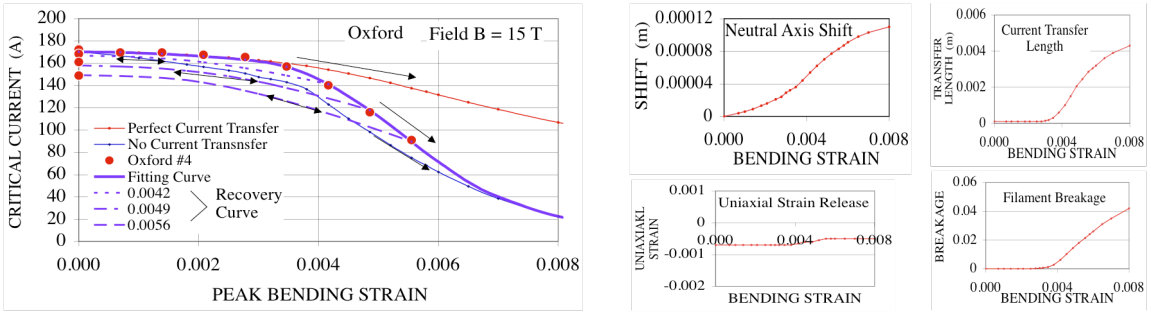

(a) Oxford wire

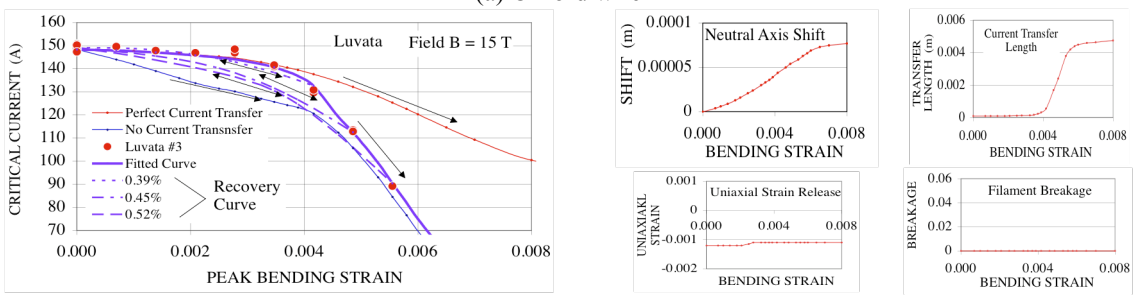

(b) Luvata wire

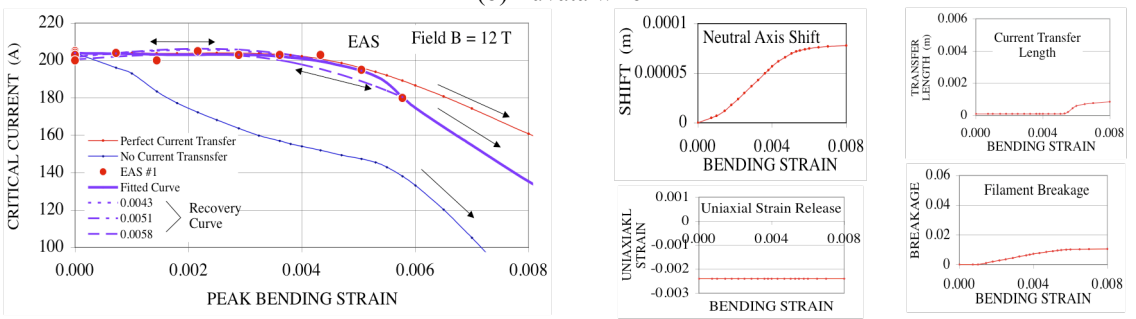

(c) EU EAS wire

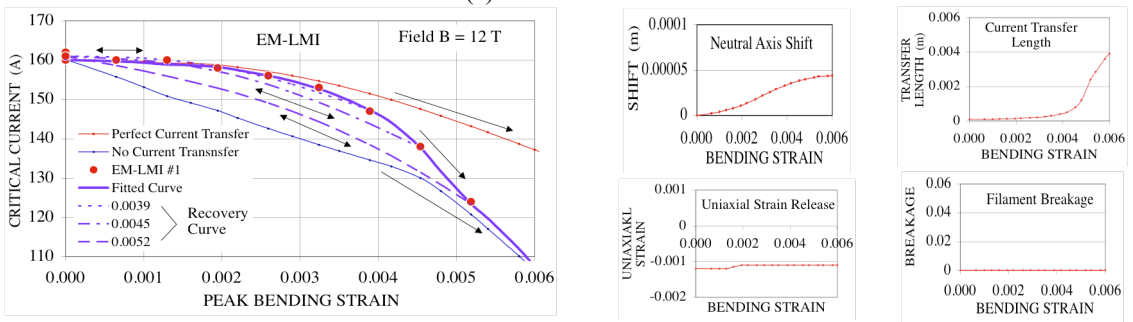

(d) EU EM-LMI wire

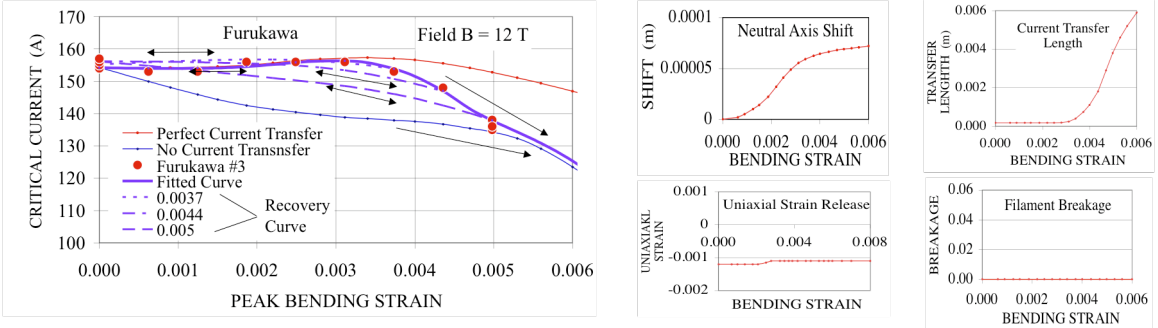

(e) JA Furukawa wire

FIGURE. 5 Critical currents of five tested wires. The solid circles in each figure are the experimental results compared with model calculation curves (left) using estimated behaviors of the four effect parameters; the neutral axis shift, the current transfer length, the filament breakage and the uniaxial strain release (right).

CONCLUSIONS

The critical currents of the internal tin wires were degraded by 47% for Oxford wire and 40% for Luvata wire at the 0.56% peak bending bending strains, and 30% for EM-LMI wires at the 0.52% peak bending strains. Higher current density wire such as the Oxford wire seems to degrade more than lower current density wires. On the other hand bronze wires of EAS and Furukawa both degraded by only about 10%. After about 0.5% peak bending, Oxford, Luvata and ESA wires showed 13%, 1.3% and 2% irreversible permanent degradation of their initial critical current values, respectively. However, the critical currents of EM-LMI and Furukawa wires were slightly increased gradually at zero bending strain after each bending cycle. It was found that the Furukawa wire showed clear improvements of the critical currents at the peak bending of around 0.3%.

The experimental behaviors of the critical currents due to pure bending have been evaluated with the four effects; the neutral axis shift, the current transfer length, the filament breakage and the uniaxial strain release. The neutral axis shift increases the critical current under small bending strains (~0.3%), but does not change the critical current at zero bending state. The current transfer length reduces the critical current with increasing the ratio of the current transfer length and the twist pitch length. The current transfer length effect seems to be an important factor which is a function of the n-value of the superconductor and the transverse resistance of the matrix. A strand having a longer twist pitch has a smaller effect due to the current transfer length. Longer strand twist pitch is desired although it is typically harmful for AC coupling losses. The filament breakage reflects an irreversible permanent degradation. The filament breakage could result in significant degradation for a strand having a long current transfer length (short twist pitch). The uniaxial strain release (reduction of thermally induced strain) causes enhancement of the critical current. Further investigations of both electrical and mechanical properties of superconducting wires under bending are desired.

ACKNOWLEDGEMENTS

This work was supported by the U.S. Department of Energy, and the US ITER Project Office. A portion of this work was performed at the National Magnetic Field Laboratory, Florida State University.

REFERENCES

1. Harris, D.L. et al., *Adv. Cryo. Eng*., **54**, Plenum, N.Y., 2008, pp. 341-348.
2. Bottura, L. et al., CERN-ITER collaboration report, Version 2, April 2008.
3. Ekin, J.W., Proceedings of the tropical conference on A15 superconductors, Ed by M. Suenaga and A. Clark, Plenum Press, New York, 1980, pp. 187-203.
4. Mitchell, N., *Cryogenics*, **43**, 2003, pp. 255-270.
5. Nijhuis, A. and Ilyin, Y. , *Supercon. Sci. Technol*. **19**, 2006, pp. 945-962.
6. Nijhuis, A. et al., *Supercon. Sci. Technol*. **19**, 2006, pp. 1136-1145.
7. Koizumi, N. et al., *IEEE Trans. Appl. Supercond*. **16**, 2006, pp. 831-834.
8. Kaiho, K., et al., *Appl. Phys. Lett*. **36**, 1980, pp. 223-225.
9. Kubo, Y. and Ozawa, T., *Journal of the Cryogenic Society of Japan*, **37**, 2002, pp. 68-76.
10. Jewell, M.C. et al., *Supercond Sci Technol*, **16**, 2003, pp. 1005-1011.
11. Miyoshi, K. et al., *Adv. Cryo. Eng*., **52**, Plenum, N.Y., 2006, pp. 536-543.
12. Ekin, J. *J. Appl. phys*. **49**, 1978, pp. 3406-3409.
13. Ekin, J. and Clark, A.F., *J. Appl. phys*. **49**, 1978, pp. 3410-3412.
14. Takayasu, M. et al., MIT Plasma Science and Fusion Center Report, PSFC/JA-08-41, 2008.
15. Nijhuis, A., *Supercond Sci Technol*, **21**, 2008, pp. 1-15.
16. Ilyin, Y. et al., *Supercond. Sci. Technol*. **20**, 2007, pp. 186–191.
17. Taylor, D.M.J. and Hampshire, D.P., *Supercond. Sci. Technol*. **18**, 2005, pp. S241–S252.